



A novel optical power-limiter-stabilizer candidate: Two-photon active chromophores derived from thiazolothiazole

Rizki R. Saputra^{1,*}, Novia E. Setyatama², Muhammad D. Ramadhan³, Mahathir M. E. Raharjo⁴, Jeddah Yanti⁵ and Dianisa K. Sandi⁶

¹Faculty of Mathematics and Natural Sciences, University of Palangka Raya, Palangka Raya, Indonesia

²College of Sciences, National Central University, Taoyuan, Taiwan

³Clean Energy Research Center, Korea Institute of Science and Technology, Seoul, South Korea

⁴Faculty of Mathematics and Natural Sciences, University of Brawijaya, Malang, Indonesia

⁵Faculty of Mathematics and Natural Sciences, Universitas Negeri Makassar, Makassar, Indonesia

⁶Faculty of Mathematics and Natural Sciences, Universitas Sebelas Maret, Surakarta, Indonesia

*Corresponding author: rizkirachmads@mipa.upr.ac.id

Received 13 February 2023

Revised 22 February 2023

Accepted 27 March 2023

Abstract

Thiazolo[5,4-d]thiazole (TTz) was exploited as the electron-acceptor, diphenylamine as the electron-donor, and fluorene/fluorene-thiophene as the electron-bridge to create two new donor-acceptor-donor (D-A-D) type chromophores, 2DFL-TTz and 2DFL-Th-TTz. The structural characteristics of the chromophores were determined using UV spectroscopy, ¹H and ¹³C NMR, and mass spectroscopic methods. Their linear and nonlinear optical properties were determined using Fluoromax. The outcomes showed that under femtosecond laser irradiation at 800 nm, the 2DFL-Th-TTz compound displayed robust two-photon induced fluorescence. The two-photon excited fluorescence (2PEF) technique was employed to map the two-photon absorption spectra of 2DFL-Th-TTz. The findings showed that this chromophore displayed strong two-photon activity (>500 GM) in the 680-850 nm spectral range, making it a possible candidate for an optical power limiter or optical power stabilizer.

Keywords: Two-photon absorption, Two-photon-induced fluorescence, Optical power-limiting, Thiazolothiazole

1. Introduction

The fast-growing development of photonic materials in the last decade can be accompanied by optical applications. Notably, organic materials with significant two-photon absorption (2PA) have been fascinating because of many practical applications based on nonlinear optical phenomena, including bio-imaging, photodynamic therapy, optical data storage, and optical power-limiting [1,2]. 2PA is a nonlinear optics (NLO) effect in which a material absorbs two photons simultaneously to reach an excited state. The gap between the ground and excited states typically results in 2PA when it is larger than the energy of one photon but smaller than that of two photons [3]. The high 2PA properties of organic materials are mainly exhibited by molecular design strategies with strong electron-acceptors and electron-donating functional groups and the intramolecular charge transfer (ICT) features in the excited state, which is related to the π -electrons conjugation system along the length of the molecule. The ICT properties are influenced by molecular planarity because electronic interactions of molecules are maximized in a planar framework [4-6]. However, in recent years, most of the reported 2PA chromophores have been confounded by decreased fluorescence quantum yield and heat-instability and photo-instability problems [6,7].

2PA material is promising for optical power-limiting applications. To obtain perfect optical power-limiting applications, 2PA materials must have high stability properties and a short reaction time. When incident light

energy increases, the material penetration rate must be reduced immediately to achieve a protective effect. Currently, 2PA materials commonly used include carbon nanotubes [8,9] and fullerenes [10-12]. However, these materials have the disadvantage of limited optical power-limited explicitly to appreciable intensities (approximately or higher than 100 W/cm²). Thus, to protect objects that are only able to withstand very low light intensity, these materials become useless. Several materials, such as phthalocyanine or metalloporphyrin, can work in low light intensity but lack stability. However, there is some indication from infrared investigations that the porphyrin ring loses a significant amount of electron density when it interacts with the acceptors [13]. Therefore, scientists must develop 2PA materials with large near-infrared band spectra, high fluorescence yields, and good stability.

Thiazolo[5,4-d]thiazole (TTz) has attracted attention due to its highly fluorescent and excellent performance in photovoltaics [14]. TTz has been actively utilized for 2PA active materials as nonlinear optical chromophores fluorescent chemosensors [15], sensing and bio-imaging applications [16], etc. Due to the imine (C=N⁺) backbone, TTz has a stiff, planar structure and is an electron-accepting fused heterocycle, lowering the tiny molecule's LUMO level. As a result, small molecules or polymers that incorporate the TTz moiety exhibit high ICT mobility and good photochemical stability [16-18]. In a recent study, researchers have developed small molecules with TTz as an acceptor unit and diphenylamine (DPA) as a donor unit. The result revealed that the DPA unit could enhance the absorption spectra and reduce HOMO energy levels. Due to its electron acceptor fused unit following the electron-withdrawing nitrogen of imine, thiazolothiazole has been considered. The stiff and coplanar structure is another justification. According to Pei-cheng et al. [19], T1 has a viable organic solar cell semi-transparently coated on building glasses, a reasonably high PCE (3.73%), and narrow absorption. The study team even conducted a series of D-A-D using triphenylamine as the donor unit and thiazolothiazole as the receptor unit.

Molecular design donor-acceptor-donor (D-A-D) based on TTz and DPA is proposed as a promising candidate for the high properties of 2PA. However, improving molecular design is needed to enhance 2PA properties. Therefore, a new design that can extend π -conjugation as a bridge unit inserted by the molecules to obtain D- π - A- π -D design must be done. Fluorene and thiophene are used as bridge units because of their unique π -conjugation [6,20]. The π -conjugated system between the electron-donating (D) and electron-accepting (A) group facilitates the intramolecular charge transfer (ICT) properties [16]. In this work, we synthesized TTz as the acceptor unit, DPA as the donor unit, and fluorene as the bridge to obtain 2DFL-TTz and 2DFL-Th-TTz. Both compounds were designed as symmetric compounds with a D- π -A- π -D model. This strategy has the advantage of inserting DPA as electron donating into the TTz core, bringing out a dual effect. Their strong electron-donating is favorable to enhancing intramolecular charge transfer (ICT). Besides, multiple noncovalent interactions form between the thiazolothiazole core and the bridging thiophene group, which can increase the planarity and rigidity, inserting fluorene as the bridge to extend π -conjugation. The appending alkyl chains in fluorene can increase the solubility of those compounds. These two symmetric compounds should be promising candidates for high properties of 2PA materials for optical power-limiting.

2. Materials and methods

The synthesis of 2DFL-TTz and 2DFL-Th-TTz compounds started from the starting material of fluorene. The steps of reactions are presented in Figure 1. Fluorene was transformed to Compound 2 (2,7-dibromo-9H-fluorene) for the first stage using a bromination reaction. Next, an alkylation reaction was performed on compound (2) to obtain Compound 3 (2,7-dibromo-9,9-dihexyl-9H-fluorene). Next, an amination process was completed on Compound 3 to obtain Compound 4 (bromo-9,9-dihexyl-N,N-diphenyl-9H-fluorene-2-amine). Then, Compound 4 was transformed into boronic intermediate Compound 5 (9,9-dihexyl-N,N-diphenyl-7-(4,4,5,5-tetramethyl-1,3,2-dioxaborolan-2-yl)-9H-fluoren-2-amine). Afterward, Compound 5 was attached to the thiophene unit with a Suzuki-Miyaura reaction to obtain Compound 6 [5-(7-(diphenylamino)-9,9-dihexyl-9H-fluoren-2-yl) thiophene-2-carbaldehyde]. At the same time, Compound 7 was already synthesized or available. In the final step, a cyclization reaction was performed on each Compound 6 and Compound 7 to form thiazolothiazole cyclic to obtain target compounds of 2DFL-TTz (Compound 1a) and 2DFL-Th-TTz (Compound 1b).

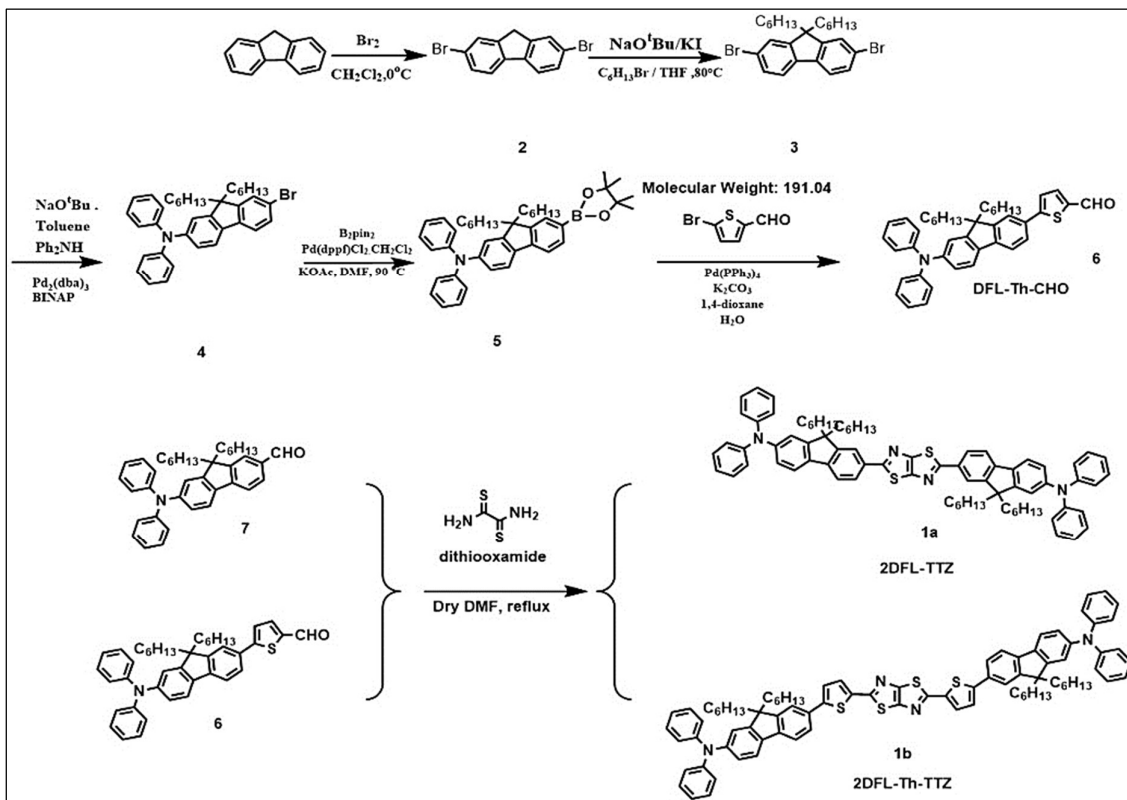


Figure 1 Schematic of synthesized thiazolothiazole derivatives. (Numbered compounds can be seen in the synthesis experiment).

2.1 Equipment/tool/material

The materials used in this experiment included fluorene, Br₂, NaHSO₃, KI, bromobutane, pyridine, diphenylamine, potassium acetate, sodium tert-butoxide, bispinacolato diboron, 5-bromothiophene-2-carboxaldehyde, dithiooxamide, N,N-dimethylmethanamide, dioxane, water, dichloromethane, tetrahydrofuran, n-hexane, hydrochloric acid, ethyl acetate, toluene, K₂CO₃, Pd(dba)₃, MgSO₄, (Pd(dppf)Cl₂CH₂Cl₂), Pd(PPh₃)₄, 2,2'-bis(diphenylphosphino)-1,1'-binaphthyl (BINAP).

Nuclear magnetic resonance (NMR) spectra were recorded on Bruker BioSpin AVANCE III at 500 MHz and JEOL-FT NMR at 300 MHz with TMS as the internal standard using CDCl₃ as a deuterated solvent. Chemical shift (δ) was stated in part per million (ppm) using residual solvent signals as internal standards. High-resolution mass spectra (HRMS) of compounds were recorded on Bruker LC-MS micrOTOF II spectrometer. The absorption measurement was carried out by UV-3500 SHIMADZU UV/VIS/NIR spectrometer with a quartz cuvette (path length = 1 cm). The fluorescence measurement was performed on the Jobin-Yvon FloroMax-4 spectrometer for the calculation of quantum yield and Jobin-Yvon FloroMax-4 spectrometer with time-correlated single-photon counting (TCSPC) accessories (FloroHub-B + Nano LED laser ($\lambda_{\text{max}} = 404$ nm) for the lifetime.

2.2 Synthesis experiment

2.2.1 Synthesis of compound 2 (2,7-dibromo-9H-fluorene)

A mixture of fluorene (5 g; 0.03 mol) dissolved in 100 mL DCM was added to bromine (3.1; 0.06 mol) by dropping wisely and stirring at 0°C (on ice bath) for 5 h (on the top condenser assembled balloon that contained nitrogen gas). The solution above was quenched with NaHSO₃ (aq) and mixed at room temperature for 1 h. The color has changed from red to pale yellow. Then, the solution was extracted with DCM and water, the organic layer was collected, and the solvent was detached by a Rotary Evaporator. The solid was stirred at ambient temperature with methanol for 30 min. The solid was filtered and dried in a vacuum oven. The product obtained was a white solid (8.74 g; 89.51%). ¹H-NMR (300 MHz, CDCl₃) δ (ppm): 7.65 (s, 2H, H₂, H₁₁), 7.59 (d, J = 8.1, 2H, H₅, H₈), 7.49-7.45 (dd, J = 8.1 Hz, 1.5 Hz, 2H, H₄, H₉), 3.85 (s, 2H, H₁₃); ¹³C-NMR (75 MHz, CDCl₃) δ (ppm): 144.77, 140.97, 140.71, 140.48, 139.68, 128.90.

2.2.2 Synthesis of compound 3 (2,7-dibromo-9,9-dihexyl-9H-fluorene)

A mixture of Compound 2 (5 g; 0.053 mol) in THF (20 mL) was added with NaO*t*Bu (5.93 g; 0.06 mol) and KI (0.03 g; 15×10^{-3} mol) and mixed reflux for 30 min. After being cooled down, the bromobutane was given into the mixture by dropping wisely and refluxed at 85°C overnight. The reaction was stopped and cooled down, and then the solution was added by pyridine (7 mL) and heated up for 1 h. The mixture was quenched with 1 N HCl until neutral and stirred at ambient temperature. Afterward, the solution was extracted using EA/brine, the organic layer was collected and dried over MgSO₄, and the solvent was removed by a rotary evaporator. The product resulted in the crude that was then purified by column chromatography using hexane as eluent. The product was a white solid (6.67 g; 87.97%). ¹H-NMR (300 MHz, CDCl₃) δ (ppm): 7.53-7.50 (d, *J* = 7.2, 2H, H5, H8), 7.46-7.44 (m, 4H, H2, H4, H9, H11), 2.01-1.83 (m, 4H, Hf), 1.39-1.13 (m, 12H Hc Hd He), 0.82-0.77 (m, 6H, Ha), 0.66 (s, 4H, Hb); ¹³C-NMR (75 MHz, CDCl₃) δ(ppm): 145.19, 142.83, 140.68, 130.14, 129.86, 128.24, 127.11, 126.94, 125.05, 121.10, 120.45, 119.93, 26.74; ¹³C-NMR (75 MHz, CDCl₃) δ(ppm): 144.77, 140.97, 140.71, 140.48, 139.68, 128.90, 40.12 (Cf), 31.47 (Ce), 29.54 (Cd), 23.68 (Cc), 22.53 (Cb) 14.01 (Ca).

2.2.3 Synthesis of compound 4 (bromo-9,9-dihexyl-*N,N*-diphenyl-9H-fluoren-2-amine)

A mixture of compound 3 (30g; 0.06 mol), diphenylamine (11.34g 0.067 mol) in toluene (120 mL) was added with BINAP (1.14g: 1.8 mmol), Pd(dba)₃ (0.56g: 0.6 mmol), sodium tetra butoxide (8.2g: 0.084 mol). Then, the mixture was cooled to ambient temperature after being stirred for 24 h at 80°C in an argon environment. The water was given to the mixture of around 100 mL. The solvent was removed by a rotary evaporator after being extracted with ethyl acetate and dried over MgSO₄. The crude product was subsequently refined using column chromatography on silica gel with hexane as the eluent. The final product of pale-yellow oil (19.44g; 55%). ¹H-NMR (300 MHz, CDCl₃) δ(ppm): 7.50-7.47 (d, *J* = 8.1Hz, 1H, H12) 743-7.40 (d, *J* = 8.1Hz, 1H, H9). 7.39-7.37 (m, 2H, H15, H13), 7.24-7.17 (m, 4H, H2), 7.10 (m, 6H, H1, H3), 7.41(m, 2H, H8, H6), 2.01-1.83 (m, 4H, Hf), 1.39-1.13 (m, 12H Hc Hd He), 0.82-0.77 (m, 6H, Ha), 0.66 (s, 4H, Hb) ¹³C-NMR (75 MHz, CDCl₃) δ(ppm): 152.79 (C16) 151.67 (C5), 147.82 (C4), 147.49 (C7), 139.88 (C11), 135.00 (C10), 129.87 (C15), 129.13 (C2), 125.89 (C9), 123.41 (C3), 123.58 (C12), 121.75 (C1), 120.43 (C6), 120.36 (C8), 120.14 (C14), 119.01 (C13), 55.30 (Cg), 40.12 (Cf), 31.47 (Ce), 29.54 (Cd), 23.68 (Cc), 22.53 (Cb) 14.01 (Ca).

2.2.4 Synthesis of compound 5 (9,9-dihexyl-*N,N*-diphenyl-7-(4,4,5,5-tetramethyl-1,3,2-dioxaborolan-2-yl)-9H-fluoren-2-amine)

A mixture of compound 4 (3 g, 5×10^{-3} mol) in three necks round bottle flask was added with KOAc (1.213 g, 0.0155 mol), bispinacolato diboron (1.7056 g, 6.71×10^{-3} mol), Pd(dppf)Cl₂.CH₂Cl₂ (0.25 g, 3.099×10^{-4} mol), and DMF (30 mL). The mixture was refluxed overnight at 90°C while being stirred, and then the solution was cooled to ambient temperature. The crude product was added to 100 mL brine solution after the solution was filtered to remove the catalyst. Then, the solution was extracted using ethyl acetate and dried over MgSO₄. The crude product was decontaminated after the solvent was removed using column chromatography on silica gel with EA/hexane 1/100 as the eluent. The result was final product was a pale-yellow powder 70% yield. ¹H-NMR (500 MHz, CDCl₃) δ(ppm): 7.84-7.82 (d, *J* = 7.5Hz, 1H, H12), 7.75 (d, *J* = 8.25 Hz, 1H, H9), 7.66-7.62 (m, 2H, H15, H13), 7.30-7.25 (m, 4H, H2), 7.20-7.10 (m, 6H, H1, H3), 7.10-7.00 (m, 2H, H8, H6), 2.01-1.83 (m, 4H, Hf), 1.45-1.42 (s, 12H, Hh), 1.39-1.13 (m, 12H Hc Hd He), 0.82-0.77 (m, 6H, Ha), 0.66 (s, 4H, Hb) ¹³C-NMR (125 MHz, CDCl₃) δ(ppm): 152.71 (C16) 149.75 (C5), 147.92 (C4), 147.48 (C7), 143.90 (C11), 135.60 (C10), 133.77 (C15), 129.11 (C2), 128.89 (C9), 123.79 (C3), 123.37 (C12), 122.46 (C1), 120.76 (C6), 119.25 (C8), 11.36 (C14), 119.01 (C13), 83.59 (Ch), 55.30 (Cg), 40.12 (Cf), 31.47 (Ce), 29.54 (Cd), 23.68 (Cc), 22.53 (Cb) 14.01 (Ca).

2.2.5 Synthesis of compound 6 (5-(7-(diphenylamino)-9,9-dihexyl-9H-fluoren-2-yl)thiophene-2-carbaldehyde)

A mixture of compound 5 (3 g; 4.77×10^{-3} mol) in dioxane was given with 5-bromothiophene-2-carboxaldehyde (1.1 g; 4.77×10^{-3} mol), K₂CO₃ (2.63 g; 0.020 mol) dissolved in water, Pd (PPh₃)₄ 0.27 g (2.39 $\times 10^{-4}$ mol). They were mixed and refluxed for 12 h and cooled to room temperature. The solution was strained to eliminate the catalyst, and water was poured into the solution. Ethyl acetate was used to extract it, after which it was dried over MgSO₄, and the solvent was drained. The crude product was decontaminated using column chromatography on silica gel and hexane to produce the finished product, as the eluent was a yellow powder with 92% yield. ¹H-NMR (500 MHz, CDCl₃) δ(ppm): 9.92 (s, 1H, Hh), 7.79-7.78 (d, *J* = 4Hz, 1H, H12), 7.67-65 (H19 H18), 7.10-7.00 (*J* = 7.5 Hz, d, 2H, H15, H13), 7.50-7.45 (d, 1H, H9), 7.30-7.25 (*J* = 7.5 Hz, m, 4H, H2), 7.20-7.14 (m, 4H, H3, H6), 7.20-7.14 (*J* = 7.5, m, 4H, H3, H6), 2.01-1.83 (m, 4H, Hf), 1.39-1.13 (m, 12H Hc Hd He), 0.82-0.77 (m, 6H, Ha), 0.66 (s, 4H, Hb) ¹³C-NMR (125 MHz, CDCl₃) δ(ppm): 182.64 (Ch), 155.71 (C17), 152.62 (C5), 151.724 (C16), 147.92 (C7), 147.86 (C4), 142.67 (C20), 141.79 (C11), 135.60 (C10), 130.88 (C14), 129.23

(C2), 125.57 (C15), 124.79 (C3), 123.57 (C18), 123.32 (C9), 122.79 (C1), 120.81 (C12), 120.48 (C8), 119.64 (C13), 118.96 (C6), 55.30 (Cg), 40.12 (Cf), 31.47 (Ce), 29.54 (Cd), 23.68 (Cc), 22.53 (Cb), 14.01 (Ca). EI-HRMS m/z calcd for $C_{42}H_{45}NOS$ 611.32, found 611.3173.

2.2.6 Synthesis of compound 1a (7,7'-(thiazolo[5,4-d]thiazole-2,5-diyl)bis(9,9-dihexyl-N,N-diphenyl-9H-fluoren-2-amine)

A mixture 7-(diphenylamino)-9,9-dihexyl-9H-fluorene-2-carbaldehyde (compound 7) (1 g; 9.47×10^{-4} mol) was given with 0.11 g dithiooxamide (1.58×10^{-3} mol) that had been purged with Argon. Dry DMF 10 mL was poured, mixed, and refluxed for 12 h (on the top condenser-assembled balloon that contained Ar gas). The solution was subsequently cooled to ambient temperature. The reaction mixture received of brine. Following that, the solution was extracted with DCM and dried over $MgSO_4$. The crude product was decontaminated by recrystallizing with pure hexane after the solvent was removed to produce the finished material, a yellow powder 38.28% yield. 1H -NMR (500 MHz, $CDCl_3$) δ (ppm): 7.96 (s, 2H, H15), 7.92-7.91 (J = 8 Hz, dd, 2H H13), 7.67-7.65 (J = 7.5 Hz, d, 2H, H12), 7.60-7.58 (J = 7.58 Hz, d, 2H, H9), 7.27-7.24 (m, 8H, H2), 7.14-7.12 (J = 8 Hz, d, 10H, H6, H3), 7.04-7.12 (J = 7.5 Hz, t, 6H, H1, H8), 2.02-1.84 (m, 8H, Hf), 1.15-1.11 (m, 24H, Hc, Hd, He), 0.82-0.77 (J = 7 Hz, t, 12H, Ha), 0.86-0.60 (m, 8H, Hb). ^{13}C -NMR (125 MHz, $CDCl_3$) δ (ppm): 169.72 (C17), 152.90 (C5), 151.66 (C16), 150.58 (C7), 148.06 (C11), 147.86 (C4), 143.80 (C10), 135.01 (C18, C19), 131.94 (C14), 129.24 (C2), 125.90 (C15), 124.12 (C3), 123.30 (C9), 122.82 (C1), 120.98 (C12), 120.29 (C8), 119.52 (C13), 118.89 (C6), 55.39 (Cg), 40.19 (Cf), 31.53 (Ce), 29.59 (Cd), 23.82 (Cc), 22.55 (Cb), 14.01 (Ca). EI-HRMS m/z calcd for $C_{78}H_{89}N_4S_2$ 1140.61 found 1140.6133.

2.2.7 Synthesis of compound 1b (7,7'-(thiazolo[5,4-d]thiazole-2,5-diyl)bis(thiophene-5,2-diyl))bis(9,9-dihexyl-N,N-diphenyl-9H-fluoren-2-amine)

A mixture of compound 6 (2 g; 3.16×10^{-3} mol) was added with 0.19 g dithiooxamide (1.58×10^{-3} mol) that had been purged with Ar. Dry DMF 20 mL was given, mixed, and refluxed for 12 h (on the top condenser-assembled balloon that contained Argon gas). After that, the solution was cooled down to ambient temperature. Enough amount of brine was carried out to the mixture, extracted with DCM, and dried over $MgSO_4$. After eliminating the solvent, the crude product was purified through recrystallization with pure EA to yield a dark red powder of 15.38% yield. 1H -NMR (500 MHz, $CDCl_3$) δ (ppm): 7.62 (s, 4H, H15, H12), 7.57-7.75 (4H, H13, H19), 7.37-7.36 (J = 4 Hz, d, 2H, H18), 7.27-7.24 (J = 7.75 Hz, t, 10H, H9, H2), 7.14-7.12 (J = 8 Hz, d, 10H, H6, H3), 7.04-7.11 (J = 7.5 Hz, t, 6H, H1, H8), 1.94-1.85 (m, 8H, Hf), 1.15-1.07 (m, 24H, He, Hd, Hc), 0.81-0.79 (J = 7 Hz, t, 12H, Ha), 0.66 (s, 8H, Hb). ^{13}C -NMR (125 MHz, $CDCl_3$) δ: 162.32 (C21), 152.52 (C5), 151.67 (C16), 149.89 (C7), 148.53 (C4), 147.95 (C20), 141.61 (C11), 141.60 (C10), 135.74 (C23), 135.43 (C22), 131.38 (C14), 129.24 (C2), 127.71 (C19), 125.90 (C17), 124.89 (C15), 124.00 (C3), 123.50 (C18), 123.46 (C9), 122.70 (C1), 120.66 (C12), 120.04 (C8), 119.65 (C13), 119.14 (C6), 55.30 (Cg), 40.12 (Cf), 31.47 (Ce), 29.54 (Cd), 23.68 (Cc), 22.53 (Cb) 14.01 (Ca). EI-HRMS m/z calcd for $C_{86}H_{88}N_4S_4$ 1304.59 found 1305.4444.

2.3. Measuring optical instruments and methods

In the solution phase, the compounds' optical characteristics were assessed. The measurement included the fluorescence quantum yield, fluorescence lifetime, and absorption and fluorescence spectra.

2.3.1 Linear optical measurements

The light source illuminates the linear absorption spectrum molecules, and the light is absorbed by the electrons in the ground states. The transition to the excited state, the molecular structure, and the conjugate length will affect the energy level of the ground states and the excited states and also change the number of absorption bands and peaks, the waveform, and the maximum absorption wavelength.

2.3.2 Absorption measurement

The absorption spectrum of the materials was measured using a Shimadzu Model 3150 UV/VIS/NIR spectrometer over the wavelength range of 200-1200 nm. Beer-Lambert law can be used for absorption measurement

$$A = \epsilon \times b \times c \quad (1)$$

where A is the measured absorbance, ϵ denotes the wavelength-dependent molar absorptivity coefficient with units of $M^{-1} \text{ cm}^{-1}$, b denotes the light path, and c represents the analyte concentration. The sample concentration to be tested was 10^{-5} M (Compound 1a) and 10^{-6} M (Compound 1b) in toluene, respectively.

2.3.3 Emission measurement

After the linear fluorescence spectrum is irradiated by the incident light of the excitation wavelength, the meson absorbs the photon to the vibrational energy level in the excited state. Because the excited state is unstable, it quickly returns to the ground state via vibration and light emission. Since the power of the light source is low, only one photon can be absorbed into the excited state at a time, so the released fluorescence is then called single-photon fluorescence. The fluorescence spectrometer used was Jobin Yvon / FluoroMax-4. The fluorescence spectrum was measured at an angle of 90 degrees. The sample concentration to be tested was 10^{-5} M (Compound 1a) and 10^{-6} M (Compound 1b) in toluene.

2.3.4 Fluorescence Quantum Yield

Fluorescence quantum yield refers to the ratio between the number of excited and luminescent molecules and the number of excited molecules. The ratio is used to assess the material's fluorescence luminescence qualities. To determine the fluorescence quantum yield, a Jobin Yvon/FluoroMax-4 fluorescence spectrometer with an integrating sphere was used. The inside of the integrating sphere is Baso. The coating can make the internal reflectance greater than 98%, so the fluorescence of the four-sided reflection can be received to measure the fluorescence quantum yield. The excitation wavelength was measured by Shimadzu 3150 UV/VIS/NIR spectrometer. The measured wavelength of the red shift in the absorption spectrum was used as the excitation sample.

The sample concentration is different every time. The concentration preparation basis was adjusted by the absorbance controlled between 0.18-0.25. The fluorescence quantum yield can be obtained as follows

$$\varphi_F = \frac{E_c - E_a}{L_a - L_c} \times 100\% \quad (2)$$

where φ_F is fluorescence quantum yield, E_c is the integral fluorescence value collected inside the integrating sphere after the light source passes through the sample. E_a is the integral fluorescence intensity value generated by the light source directly injected into the integrating sphere. L_a is the incident light intensity integral value of the unpassed sample, and L_c is the incident light integral value of the irradiated sample.

2.3.5 Fluorescence lifetime

Fluorescence lifetime is the time when the electron stays in the excited state. Jobin Yvon FluoroMax-4 fluorescence spectrometer with Fluorollub Pulse LED and 404 nm laser head as the excitation light source was used to achieve the fluorescence lifetime at an angle of 90°. The sample concentration to be tested was 10^{-5} M (Compound 1a) and 10^{-6} M (Compound 1b) in toluene.

2.3.6 Nonlinear Optical Measurements

The laboratory used a Ti-sapphire laser (Chameleon Ultra 11, Coherent) as the excitation source with an average power of 3.5 W, a laser pulse width of 140 fs, a repetition rate of 80 MHz, and a beam diameter of 2 mm, and an adjustable wavelength range from 680 nm to 1080 nm (Figure 2).

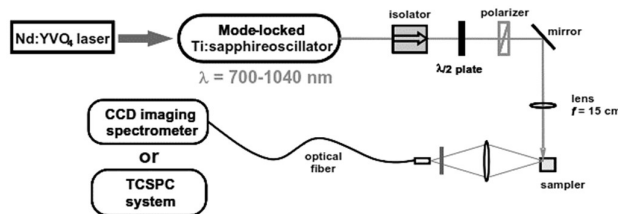


Figure 2 2PA measurements.

The measurement of the sample was conducted in a solution state. The model molecule does not absorb linearly between 700 nm and 1000 nm wavelengths. Therefore, if the fluorescence of the near-infrared section was used as the excitation wavelength and the fluorescence is observed, it can be inferred that the observed fluorescence is two-photon absorption. Two-photon fluorescence is caused by the mechanism.

The samples were in the solution state configured as 10^{-4} M, and the solvent was toluene. They were filled into a 1 cm x 1 cm x 3.5 cm bucket-shaped quartz plasma sample tank. The laser beam was adjusted by the Ti: sapphire laser and emitted via an isolator. The beam would not be returned to the laser host, and the mirror would be turned to a 90° angle. Then the intensity of the incident light source was controlled by a neutral filter (ND filter), and the laser beam size (diameter = 2 mm) was fixed with the iris. The lens with a focal length of 5 cm was used to focus on the sample stage where the sample was placed.

The position of the sample was outside the focus. It was also necessary to let the beam pass through the edge of the sample slot to prevent the fluorescent light from being emitted by the other unexcited. The absorption of the area was called the self-absorption effect. Therefore, to avoid the self-absorption effect, the beam was passed through the edge of the sample cell. The fiber optic cable was very close to the sample cell to receive the fluorescence and transmit it to the CCD spectrometer. Computer spectrum software can measure the fluorescence spectrum. Due to the space of the optical table and the convenience of erection, the film state was measured by placing a lens with a focal length of 5 cm. It was done after the samples' position was in the original solution state. The laser light was then collected.

The sample position was focused on. A fiber optic cable was also installed to receive the fluorescence and connect to our CCD spectrometer and the two-photon excited fluorescence spectrum. This laboratory uses the fluorescence comparison method to measure the sample in solution. Therefore, we compare it with a standard. We use DFL-OXD (Figure 3) with a concentration of 10^{-4} M in Toluene as a standard. It is a commercially available dye at 790 nm. The quantum yield is 59% with a 185 GM two-photon cross-section.

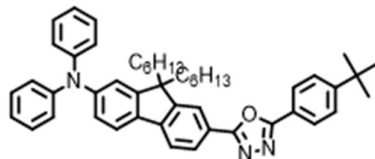


Figure 3 DFL-OXD structure.

Two nonlinear optical investigations are the primary uses of this apparatus. The first is the femtosecond time domain cross-section spectrum of two-photon absorption. At each wavelength, the measurement energy is fixed. At the nm wavelength, the measurement energy is fixed. The fluorescence spectrum obtained by excitation with different wavelengths is obtained. The fluorescence area is integrated. The quantum yield of the sample and the value of the standard DFL-OXD are brought into the calculation formula of the fluorescence comparison method to obtain each wavelength. The fluorescence comparison method is as follows

$$\delta_s = \frac{s_s}{s_r} \times \frac{\phi_r}{\phi_s} \times \frac{c_r}{c_s} \times \delta_r \quad (3)$$

where the subscripts of s and r stand for the sample and reference molecules, the fluorescence intensity was denoted as S, the quantum yield was indicated as Φ , and ϕ represents the experimental setup's overall fluorescence collection efficiency. The solution's concentration was given by c. δ_r is the reference molecule's 2PA cross-section-about 15% of the total experimental uncertainty in δ [21].

The second was an energy-dependent experiment. Because the fluorescence intensity of the two-photon material depends on the intensity of the incident light, we experimented with the best wavelength of the two-photon in the first experiment. It is easy to observe the nature of the two-photon fluorescence and then adjust the passing energy with the ND filter. After the measurement, the fluorescence spectrum of different energies at the same wavelength can be obtained, and then the fluorescence spectrum is obtained.

3. Results and discussion

3.1 Synthesis explanation

The target compounds were synthesized in several steps, as shown in Figure 2. First, a series of fluorene-based precursors was bromination using two equivalent bromines as a reagent in ice bath conditions. Compound 2 was produced as much as 90% as a white crystalline powder. Brominated fluorene was prepared for alkylation at nine

fluorene positions, making such derivatives highly soluble in common organic solvents and providing good compatibility. In this step, the deprotonation phenomenon involved KI, indicated by increased temperature when adding bromohexane. The dihexyl group was attached to the fluorene ring [22]. The alkylation step yielded 80% of Compound 3, as a white crystalline solid, purified using hexane as the eluent in a column chromatography process. A donor was introduced in the π -conjugated system, resolving the solubility issues. Diphenylamine added via amination reaction use $Pd_2(dbu)_3$ as a catalyst and BINAP as a ligand. An unstable yield was afforded in the amination step, which was possibly caused by two sites of compound 3 for amination possibility. The mole ratio of Compound 3 to diphenylamine is chosen at 1:1 to address the issue of selectivity on that step and prevent amination on two active sites [23]. As a result, one site amination product isolated Compound 4 in 51% yielded a viscous liquid. Compound 4 was freshly prepared by Miyaura reaction in DMF and reflux condition. Borylation used bis(pinacolato)diboron as the boron source to substitute the bromide's position. Fluorene-based Compound 5 was successfully obtained in 70% as a yellow crystal powder. Compound 7 was already available.

The isolated Compound 5 was prepared by Suzuki coupling from 5-bromothiophene-2-carboxaldehyde with $Pd(PPh_3)_4$ in dioxane/water (3/1, v/v), then through column chromatography as a purification method [24]. Compound 6, the thiophene-extended form of compound 7, was produced in 92% yield as a solid yellow powder. Compounds 7 and 6 were prepared for the final step by cyclization to thiazolothiazole to synthesize Compounds 1a and 1b, respectively. Dithiooxamide, as a cyclization reagent, was added to the mixture containing precursor and dry DMF. This step was air sensitive. The glassware containing all the compounds should be purged with Argon [24]. The purpose of purging is to avoid air contaminants inside the system. During the reaction, the system was assembled by a balloon that contained Argon. Compound 1a was successfully isolated in bright yellow solid (38.28%), while Compound 1b was successfully isolated in a dark red solid (15.38%) yield.

3.2 One-photon UV-vis spectral properties

The optoelectronic and fluorescence spectra in the precise solvent comprises the optical characteristics study of thiazolothiazole derivatives. The λ_{abs} and emission λ_{em} maxima were included in the analysis. The lifetimes of the studied dyes and the fluorescence quantum yield ϕ_f are described in detail and shown in Table 1. The samples' emission and absorption characteristics are shown in Figure 4. The solution photo-physical properties of TTZ derivatives were investigated in toluene (concentration = 1.0×10^{-5} M). Shimadzu 3501 UV/Vis/NIR spectrophotometer and Jobin-Yvon/FluoroMax-4 spectrometer were used to record one-photon absorption (1PA) and emission spectra.

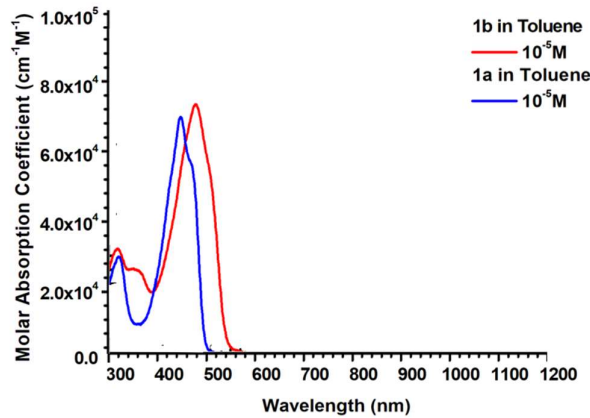


Figure 4 One-photon absorption (1PA) spectra of TTZ.

Two peaks in the 300-400 and 400-500 nm ranges could be seen in the toluene's electronic absorption spectrum (Figure 5), the exact transitions between $S_0 \rightarrow S_2$, and $S_0 \rightarrow S_1$. The compound's charge transfer (CT) transition could be employed to assist the lower energy's high absorption band. The transition entailed the transfer of one electron from the diphenylamine moiety, which donated electrons, to the thiazolothiazole, which withdrawn electrons. In Compounds 1a and 1b with a thiazolothiazole as a core, two diphenylamines were connected to fluorene for Compound 1a. Meanwhile, two diphenylamines were connected to thiophenyl fluorene for Compound 1b.

The diphenylamine group was performed as the terminal or bridge for D- π -A- π -D structural arrangement. The two dialkylfluorene units could be in an *E* or *Z* conformation. Compound 1b's absorption band showed a bathochromic shift in the absorption spectra compared to Compound 1a. It showed that the chromophores' thiophene addition in the elongate conjugation system was successful. The various charge distributions inside the

molecule could be blamed for this phenomenon. The typical push-pull system structure of these chromophores had an absorbance maximum of 437 nm for Compound 1a and 468 nm for Compound 1b. Pavia et al. [25] explained that increasing conjugation length extension could result in a bathochromic shift. The bathochromic shift observed for Compound 1b could be explained by the extended conjugation of double bonds, which would decrease the energy required for electronic excitation. In other words, a chromophore's electronic energy levels increase. The absorbance of the light was absorbed in the longer wavelength as the energy needed to shift from an occupied electronic energy level (HOMO) to an unoccupied level (LUMO) decreased. Since the shorter system of the electron acceptor (thiazolothiazole) and the electron donor (diphenylamine) in Compound 1a made charge transfer less efficient, blue-shifted molecules occurred.

The charge transfer state's one-photon absorption (1PA) strength was then associated with extended conjugation systems. For instance, Compound 1a had a little greater 1PA intensity than Compound 1b (Figure 5). The increase in the molar absorption coefficient, implied by ϵ_{max} divided by the molecular weight [26], was apparent for Compound 1b. It could be indicated by the extending π delocalization from the addition of a thiophene ring and a particular coupling between peripheral donor units in Compound 1b. The reduced ϵ_{max} of Compound 1a was enough correlated to the short length of π systems. These compound solutions emitted intense green (Compound 1a) and orange (Compound 1b) fluorescence when exposed to a long-wavelength UV lamp, consistent with the measured fluorescence spectra.

Compound 1a's emission bands could be seen in the steady-state fluorescence spectra for TTZ series chromophores in toluene at 485, 518, and 555 nm. The fluorescence bands of Compound 1b are red-shifted to 529, 566, and 615 nm. The emission has a shorter wavelength than the absorption. When an excited electron relaxes to the emissive state and releases energy through vibrational relaxation, this phenomenon occurs. An electron discharges energy less than the absorption energy utilized in excitation when it relaxes to the ground. A triple peak may be seen in the fluorescence spectra (Figure 5), which indicates that the emission involves and arises from many excited states. Significant charge redistribution occurs during excitation before emission, and the emission emanates from a substantially dipolar emissive state following Compound 1b's large stokes shift in toluene [27]. The elongated structure probably made the better delocalization of the ICT in the system. Thus, the transfer process of charge-transfer character from donor to acceptor of Compound 1b is better than Compound 1a.

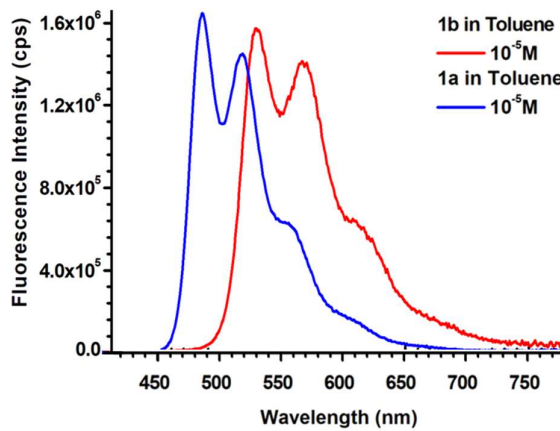


Figure 5 Fluorescence Spectra of TTZ Series in Toluene.

The chromophores investigated exhibited a modest emission in a toluene solution with quantum yields of 64.85% (Compound 1a) and (Compound 1b) 51.35%. Quantum yield is measured as the difference between the number of photons released and the number absorbed. According to the quantum yields, the longer π conjugation system in Compound 1b could be a factor in decreasing its quantum yield. The quantum yield decreased when σ -electron and π -electron were used as the elongating structure of the molecular system. These indicated that the addition of thiophene was incorporated in quantum yield. Overall, there was the peak position of the longest wavelength absorption band (λ_{max}) and the peak position of the emission spectrum (λ_{em}). Compared to compound 1a, Compound 1b was found in the longer wavelength area (Table 1). It would reduce Compound 1b's quantum yield (Φ_F) because a nonradiative path was made possible by the emitting state's lower energy. Similar findings have been reported by Zhang et al. [28]. The fluorescence lifetime is shown in Table 1. According to the maximum fluorescence intensity, the emission decay of the dyes investigated in toluene was seen at 555 nm (Compound 1a) and 615 nm (Compound 1b). The average amount of time a molecule spends in the excited state before returning to the ground state was used to calculate lifetime (generally near 10 ns). With two-exponential functions, the decay

lifetime could be properly matched, resulting in fluorescence lifetimes of 1.18 ns (Compound 1a) and 1.13 ns (Compound 1b).

Table 1 Optical properties of TTZ series in toluene.

Compound	λ_{abs} (nm) ^a	ϵ_{max} ($M^{-1}cm^{-1}$) ^b	λ_{em} (nm) ^c	ϕ_F ^d (%)	τ (ns) ^e	δ_2^{max} (GM) ^f
1a	437	0.67	485, 518, 555	64.85	1.18	-
	310					
1b	468	0.71	529, 566, 615	51.35	1.13	1294
	341					
	309					

The concentration was $1 \times 10^{-5} M$. ^aOne-photon absorption maximum, ^bMolar absorption coefficient, ^cIPA-induced fluorescence emission maximum, ^dFluorescence quantum efficiency, ^eIPA-induced fluorescence lifetime, and ^fMaximum 2PA cross-section value (with an experimental error of approximately $\pm 15\%$); 1 GM = $1 \times 10^{-50} \text{ cm}^4 \text{s}$ per photon molecule.

3.3 Nonlinear properties of TTZ series

Based on linear optical properties, Compound 1b candidate was a model chromophore with good two-photon properties. In contrast to Compound 1a, Compound 1b's absorption band depicted a bathochromic shift in the absorption spectra. It demonstrated that the elongation conjugation system's thiophene addition to the chromophores is effective. This occurrence could be attributable to the unique charge distributions present inside the molecule. Blue-shifted molecules appeared in Compound 1a due to the less effective charge transfer caused by the shorter system of the electron acceptor (thiazolothiazole) and the electron donor (diphenylamine). According to linear optical properties data, the study continued to the nonlinear optical properties (two-photon). To produce highly two-photon absorption, there were three essential parts. A polarizable bridge, a strong electron acceptor (A), and a strong electron donor (D) made this system. The D and A could function as the group's capstone or π -cores. Figure 6 (A & B) and Table 1 show Compound 1b's nonlinear optical results. The 2PA cross-section was measured utilizing a femtosecond pulse employing the two-photon-induced fluorescence measurement method, which can avoid any problems brought on by excited-state excitation.

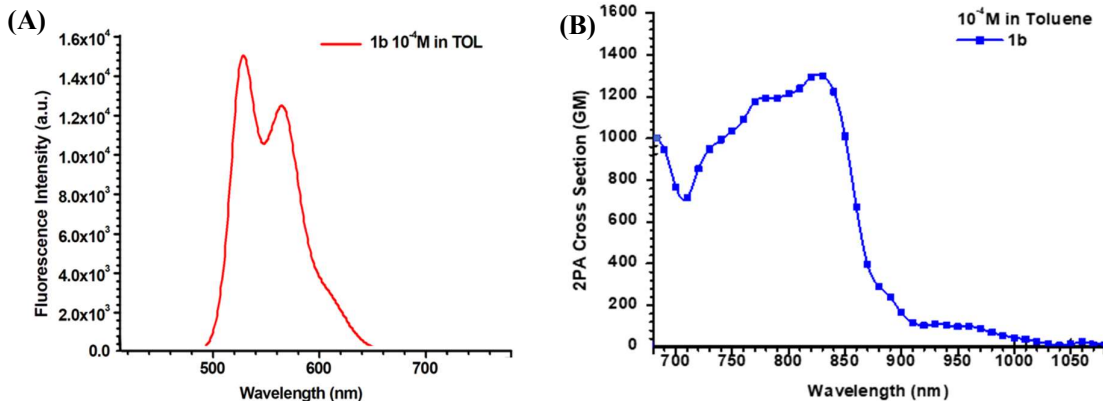


Figure 6 (A) Fluorescence Intensity and (B) 2PA Cross Section (GM) of 2 (DFL-TP)-TTZ ($1 \times 10^{-4} M$) in Toluene.

The density of states would grow when the molecular size expanded due to the extended conjugation. The ground state and two-photon allowed states were coupled with more effective channels, increasing the δ_2 over a wide range of wavelengths. Let's examine the obtained 1PA and 2PA spectra of Compound 1b. The red-shift ICT absorption band in toluene (Figure 6) may provide larger δ_2 because the narrower energy gap causes a higher chance of two-photon excitation. (Figure 4 and Figure 6). The peak positions of the 2PA maxima are significantly blue-shifted compared to the wavelength position of twice their lowest-energy linear absorption peak (i.e., λ_{max} of $2\text{PA} < 2\lambda_{\text{max}}$ of 1PA). These results revealed that the energy of the lowest permissible one-photon state of these compounds is higher than that of the accessible two-photon state. The symmetry influences the dipole moment and affects the electron transfer and the conjugated electrons in the system. The cross-section value exhibits a good 2PA-chromophore. The highest GM value of Compound 1b is 1294 GM at 830 nm. The similarity between the emission spectrum in 1PA (Figure 4) and the emission spectrum in 2PA (Figure 5) is indicated predominantly by the same excited state.

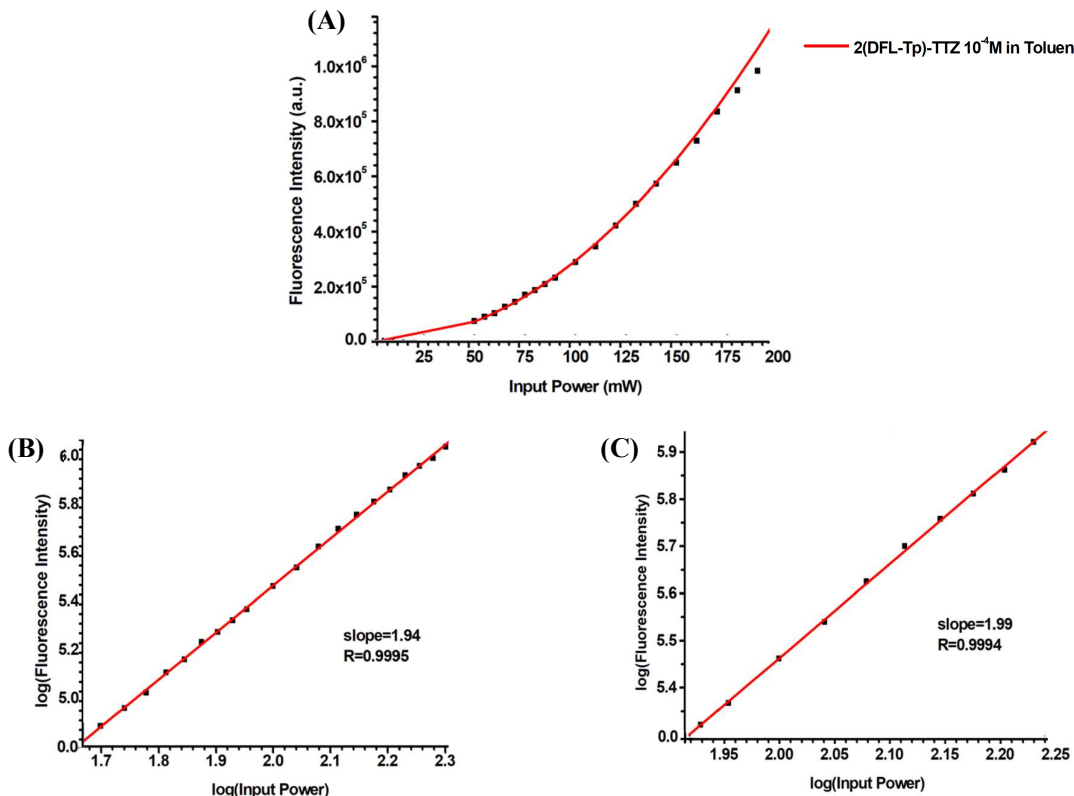


Figure 7 (A)Fluorescence intensity toward input power on range 50-200 mW and Logarithmic plots of power-squared dependence of the 2PA-induced on the differences in input power range (B) 50-200 mW and (C) 85-170 mW of 2(DFL-TP)-TTZ (1×10^{-4} M) in toluene.

Moreover, the 2PA phenomena should be confirmed to prove that the fluorescence is caused by the two-photon mechanism. Thus, energy-dependent experiments using a Ti-sapphire laser were needed. Furthermore, the wavelength in the maximum area of 2PEF was checked. These wavelengths were used to measure the power dependence. Otherwise, in power dependence measurement, the wavelength was constantly controlled by both input and output energy. This measurement was used to prove that Compound 1b process deals with the 2PA process. The excitation fluorescence and the intensity of the incident light source are plotted in two curves. The power-squared dependence of 2PA-induced fluorescence intensity on the excitation intensity is displayed in Figure 7. The slope of each logarithmic plot of Compound 1b is 1.94 and 1.99 (close to 2.0). Thus, it could be ensured that the phenomena observed, and the fluorescence is caused by two-photon fluorescence or indicative of a two-photon excitation process.

4. Conclusion

Thiazolothiazole was used as the electron acceptor, and the diphenylaminofluorene or diphenylaminofluorene-thiophene as the electron donor to create two novel chromophores. The emission maxima span a large range of wavelengths, from 450 to 750 nm. High multiphoton absorption is displayed by chromophores 1b, allowing for the simultaneous observation of the contributions of many processes. In the 800–1100 nm range, Compound 1b's greatest effective 2PA cross-section was 1294 GM. In addition, according to nonlinear optical properties, Chromophore 1b shows an excellent potential candidate for an optical power limiter or optical power stabilizer.

5. Acknowledgements

We thank Prof. Tzu-Chau Lin from the Department of Chemistry, College of Sciences, National Central University, Taiwan, for all his financial and measurement analysis support.

6. References

- [1] Yilmaz H, Küçüköz B, Sevinç G, Tekin S, Yaglioglu HG, Hayvali M, et al. The effect of charge transfer on the ultrafast and two-photon absorption properties of newly synthesized boron-dipyrromethene compounds. *Dyes Pigments*. 2013;99(3):979-985.
- [2] Lemercier G, Four M, Chevreux S. Two-photon absorption properties of 1,10-phenanthroline-based Ru(II) complexes and related functionalized nanoparticles for potential application in two-photon excitation photodynamic therapy and optical power limiting. *Coordin Chem Rev*. 2018;368:1-12.
- [3] Wang G, Bennett D, Zhang C, Coileáin C, Liang M, McEvoy N, et al. Two-photon absorption in monolayer MXenes. *Adv Opt Mater*. 2020;8(9):1902021.
- [4] Sayresmith NA, Saminathan A, Sailer JK, Patberg SM, Sandor K, Krishnan Y, et al. Photostable voltage-sensitive dyes based on simple, solvatofluorochromic, asymmetric thiazolothiazoles. *J Am Chem Soc*. 2019;141(47):18780-18790.
- [5] Rajashekhar B, Sowmendran P, Sai SSS, Rao GN. Synthesis, characterization and two-photon absorption based broadband optical limiting in diarylideneacetone derivative. *J Photoch Photobio A*. 2012;238:20-23.
- [6] Tang C, Zheng Q, Zhu H, Wang L, Chen SC, Ma E, et al. Two-photon absorption and optical power limiting properties of ladder-type tetraphenylen cored chromophores with different terminal groups. *J Mater Chem C*. 2013;1(9):1771-1780.
- [7] Li Y, Zheng M, Wang J, Gao Y, Zhang B, Yang W. Two-photon absorption and fluorescence fluoride-sensing properties of N-octyl-3,6-bis[4-(4-(diphenylamino)phenyl)phenyl]-1,4-diketo-pyrrolo[3,4-c]pyrrole. *Dyes Pigments*. 2014;104:97-101.
- [8] Torres TC, López PN, Gutiérrez MH, Valdez TM, López OJ, Terrones M. Optoelectronic modulation by multi-wall carbon nanotubes. *Nanotechnology*. 2013;24(4):045201.
- [9] Gandra N, Chiu PL, Li W, Anderson YR, Mitra S, He H, et al. Photosensitized singlet oxygen production upon two-photon excitation of single-walled carbon nanotubes and their functionalized analogues. *J Phy Chem C*. 2009;113(13):5182-5185.
- [10] Rahulan KM, Flower NAL, Sujatha RA, Padmanathan N, Gopalakrishnan C. Nonlinear optical absorption studies of CoMoO₄ hybrid nanostructures. *J Mater Sci Mater Electron*. 2018;29(2):1504-1549.
- [11] Zheng XL, Yang L, Shang B, Wang MQ, Niu Y, Li WQ, et al. Two-dimensional two-photon absorptions and third-order nonlinear optical properties of Ih fullerenes and fullerene onions. *Phys Chem Chem Phys*. 2020;22(25):14225-14235.
- [12] Yang CC, Duan X, Li L, Zheng XL, Chen J, Tian WQ, et al. BN-doped carbon nanotubes and nanoribbons as nonlinear-optical functional materials for application in second-order nonlinear optics. *ACS Appl Nano Mater*. 2023;6(3):1549-1561.
- [13] Wang ZM, Neogi A. Nanoscale photonics and optoelectronics. 1st ed. New York: Springer; 2010.
- [14] Chen Y, Du Z, Chen W, Wen S, Sun L, Liu Q, et al. New small molecules with thiazolothiazole and benzothiadiazole acceptors for solution-processed organic solar cells. *New J Chem*. 2014;38(4):1559-1564.
- [15] Jung JY, Han SJ, Chun J, Lee C, Yoon J. New thiazolothiazole derivatives as fluorescent chemosensors for Cr³⁺ and Al³⁺. *Dyes Pigments*. 2012;94(3):423-426.
- [16] Kumar V, Sony S, Kaur N, Mobin SM, Kaur P, Singh K. Thiazolothiazole based donor-π-acceptor fluorophore: Protonation/deprotonation triggered molecular switch, sensing and bio-imaging applications. *Anal Chim Acta*. 2022;1206:339776.
- [17] Lim DH, Jang SY, Kang M, Lee S, Kim YA, Heo YJ, et al. A systematic study on molecular planarity and D-A conformation in thiazolothiazole- and thiylenevinylene-based copolymers for organic field-effect transistors. *J Mater Chem C*. 2017;5(39):10126-10132.
- [18] Nazim M, Ameen S, Akhtar MS, Lee YS, Shin HS. Novel thiazolothiazole based linear chromophore for small molecule organic solar cells. *Chem Phys Lett*. 2013;574:89-93.
- [19] Cheng P, Shi Q, Lin Y, Li Y, Zhan X. Evolved structure of thiazolothiazole based small molecules towards enhanced efficiency in organic solar cells. *Org Electron*. 2013;14(2):599-606.
- [20] Amna B, Siddiqi HM, Hassan A, Ozturk T. Recent developments in the synthesis of regioregular thiophene-based conjugated polymers for electronic and optoelectronic applications using nickel and palladium-based catalytic systems. *RSC Adv*. 2020;10(8):4322-4396.
- [21] Zhang HC, Guo EQ, Zhang YL, Ren PH, Yang WJ. Donor-acceptor-substituted anthracene-centered cruciforms: synthesis, enhanced two-photon absorptions, and spatially separated frontier molecular orbitals. *Chem Mater*. 2009;21(21):5125-5135.
- [22] Lin TC, Chen YF, Hu CL, Hsu CS. Two-photon absorption and optical power limiting properties in femtosecond regime of novel multi-branched chromophores based on tri-substituted olefinic scaffolds. *J Mater Chem*. 2009;19(38):7075-7080.

- [23] Kannan R, He GS, Lin TC, Prasad PN, Vaia RA, Tan LS. Toward highly active two-photon absorbing liquids. synthesis and characterization of 1,3,5-triazine-based octupolar molecules. *Chem Mater.* 2004;16(1):185-194.
- [24] Zhu X, Tian C, Jin T, Wang J, Mahurin SM, Mei W, et al. Thiazolothiazole-linked porous organic polymers. *Chem Commun.* 2014;50(95):15055-15058.
- [25] Pavia DL, Lampman GM, Kriz GS, Vyvyan JR. *Introduction to spectroscopy.* 5th ed. Massachusetts: Cengage Learning; 2015.
- [26] Zhou H, Zheng Z, Xu G, Yu Z, Yang X, Cheng L, et al. 1, 3, 5-triazine-cored derivatives dyes containing triphenylamine based two-photon absorption: synthesis, optical characterization and bioimaging. *Dyes Pigm.* 2012;94(3):570-582.
- [27] Shao J, Guan Z, Yan Y, Jiao C, Xu QH, Chi C. Synthesis and characterizations of star-shaped octupolar triazatruxenes-based two-photon absorption chromophores. *J Org Chem.* 2011;76(3):780-790.
- [28] Zhang D, Gao Y, Dong J, Sun Q, Liu W, Xue S, et al. Two-photon absorption and piezofluorochromism of aggregation-enhanced emission 2,6-bis(p-dibutylaminostyryl)-9,10-bis(4-pyridylvinyl-2) anthracene. *Dyes Pigm.* 2015;113:307-311.